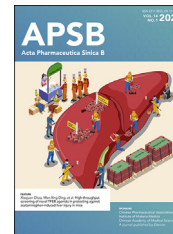




Chinese Pharmaceutical Association  
Institute of Materia Medica, Chinese Academy of Medical Sciences

Acta Pharmaceutica Sinica B

[www.elsevier.com/locate/apsb](http://www.elsevier.com/locate/apsb)  
[www.sciencedirect.com](http://www.sciencedirect.com)



ORIGINAL ARTICLE

# Cancer immunotherapy with enveloped self-amplifying mRNA CARG-2020 that modulates IL-12, IL-17 and PD-L1 pathways to prevent tumor recurrence



Ju Chen<sup>a,c,†</sup>, Bhaskara Reddy Madina<sup>b,†</sup>, Elham Ahmadi<sup>a,b,†</sup>,  
Timur Olegovich Yarovinsky<sup>b</sup>, Marie Marthe Krady<sup>b</sup>,  
Eileen Victoria Meehan<sup>a</sup>, Isabella China Wang<sup>a,d</sup>, Xiaoyang Ye<sup>a</sup>,  
Elise Pitmon<sup>a</sup>, Xian-Yong Ma<sup>b</sup>, Bijan Almassian<sup>b</sup>, Valerian Nakaar<sup>b,\*</sup>,  
Kepeng Wang<sup>a,\*</sup>

<sup>a</sup>Department of Immunology, School of Medicine, University of Connecticut Health Center, Farmington, CT 06030, USA

<sup>b</sup>CaroGen Corporation, Farmington, CT 06030, USA

<sup>c</sup>The Eighth Clinical Medical College of Guangzhou University of Chinese Medicine, Foshan Hospital of Traditional Chinese Medicine, Foshan 528000, China

<sup>d</sup>The Loomis Chaffee School, Windsor, CT 06095, USA

Received 31 May 2023; received in revised form 1 August 2023; accepted 15 August 2023

## KEY WORDS

Virus-like vesicles;  
Oncolytic virus;  
IL-12;  
IL-17;  
PD-L1;  
T cell exhaustion;  
Combination therapy;  
Cancer immunotherapy

**Abstract** Targeting multiple immune mechanisms may overcome therapy resistance and further improve cancer immunotherapy for humans. Here, we describe the application of virus-like vesicles (VLV) for delivery of three immunomodulators alone and in combination, as a promising approach for cancer immunotherapy. VLV vectors were designed to deliver single chain interleukin (IL)-12, short-hairpin RNA (shRNA) targeting programmed death ligand 1 (PD-L1), and a dominant-negative form of IL-17 receptor A (dn-IL17RA) as a single payload or as a combination payload. Intralesional delivery of the VLV vector expressing IL-12 alone, as well as the trivalent vector (designated CARG-2020) eradicated large established tumors. However, only CARG-2020 prevented tumor recurrence and provided long-term survival benefit to the tumor-bearing mice, indicating a benefit of the combined

\*Corresponding authors.

E-mail addresses: [vnakaar@carogencorp.com](mailto:vnakaar@carogencorp.com) (Valerian Nakaar), [kewang@uchc.edu](mailto:kewang@uchc.edu) (Kepeng Wang).

†These authors made equal contributions to this work.

Peer review under the responsibility of Chinese Pharmaceutical Association and Institute of Materia Medica, Chinese Academy of Medical Sciences.

<https://doi.org/10.1016/j.apsb.2023.08.034>

2211-3835 © 2024 The Authors. Published by Elsevier B.V. on behalf of Chinese Pharmaceutical Association and Institute of Materia Medica, Chinese Academy of Medical Sciences. This is an open access article under the CC BY-NC-ND license (<http://creativecommons.org/licenses/by-nc-nd/4.0/>).

immunomodulation. The abscopal effects of CARG-2020 on the non-injected contralateral tumors, as well as protection from the tumor cell re-challenge, suggest immune-mediated mechanism of protection and establishment of immunological memory. Mechanistically, CARG-2020 potentially activates Th1 immune mechanisms and inhibits expression of genes related to T cell exhaustion and cancer-promoting inflammation. The ability of CARG-2020 to prevent tumor recurrence and to provide survival benefit makes it a promising candidate for its development for human cancer immunotherapy.

© 2024 The Authors. Published by Elsevier B.V. on behalf of Chinese Pharmaceutical Association and Institute of Materia Medica, Chinese Academy of Medical Sciences. This is an open access article under the CC BY-NC-ND license (<http://creativecommons.org/licenses/by-nc-nd/4.0/>).

## 1. Introduction

Immunotherapies have provided remarkable clinical benefits to patients with different types of cancer<sup>1,2</sup>. One arm of cancer immunotherapy is the use of oncolytic viruses, which selectively replicate in the tumor microenvironment (TME) and are able to destroy cancer cells and expose tumor antigens to host immune cells<sup>3</sup>. To date, three oncolytic viruses have been approved for cancer treatment<sup>4–6</sup>. Among them, T-VEC, derived from type 1 herpes simplex virus, carries the granulocyte macrophage colony-stimulating factor (GM-CSF) to enhance systemic antitumor immune responses<sup>6</sup>. Several oncolytic viruses with transgenes that target other aspects of tumor immunity have been developed as well, with GM-CSF remaining the most popular cargo<sup>3</sup>. However, current applications of oncolytic virus treatments are still limited, in part due to the limited capacity of these agents to regulate multiple immune pathways that are critical for tumor eradication.

The virus-like vesicle (VLV) is a hybrid of components from two unrelated animal viruses, the alphavirus Semliki Forest virus (SFV) RNA-dependent polymerase and rhabdovirus vesicular stomatitis virus glycoprotein (VSV-G), that produces infectious replication-competent enveloped vesicles at high titers *in vitro*<sup>7–9</sup>. VLVs can express multiple proteins, such as reporters, antigens, and/or membrane proteins, by employing sub-genomic promoters or 2A self-cleaving peptides<sup>10–13</sup>. Delivery of VLVs *in vivo* results in transient expression of VLV-encoded proteins and induction of antigen-specific immune responses<sup>7–10,12,13</sup>. Prior applications of VLVs were focused on developing prophylactic vaccines or immunotherapy for chronic infections such as HBV or HIV<sup>8,10,12–14</sup>, but VLVs have not been explored before for use as oncolytic artificial viruses. Nor have they been used to modulate immune cell responses *via* cytokine and/or short-hairpin RNA (shRNA) delivery.

Several distinct pathways have been targeted successfully in cancer immunotherapy, combinations of which could enhance their effectiveness, especially when delivered by VLV. Systemic immune checkpoint blockade with antibodies against programmed death-1/programmed death ligand-1 (PD-1/PD-L1) and other immune pathways has demonstrated durable clinical responses and prolonged survival in patients with solid tumors, but only a minority of patients exhibit complete responses<sup>15</sup>. For example, combination therapy with anti-PD-1 antibody and anti-CTLA-4 antibody in a metastatic melanoma clinical study showed a synergistic clinical response compared to the corresponding monotherapies, but efficacy was still limited and toxicities related to systemic immune activation were of concern<sup>16</sup>. Checkpoint immunotherapy against colorectal cancer (CRC) also showed some success, but was limited to cases with microsatellite

instability (MSI)<sup>17,18</sup>. Although immune checkpoint blockade is arguably the most effective current cancer therapy approach, the overall response rate in most solid tumors is only around 20%<sup>19,20</sup>. This efficacy is limited to patients with “hot” tumors, thereby warranting an effective approach to transform “cold” tumors. Oncolytic viruses are known to modulate the TME and to convert cold tumors into hot tumors.

Another approach in immunotherapy is to target pathways that activate cancer-killing immune cells or those that regulate cancer-promoting inflammation<sup>21,22</sup>. An example of such a pro-cancer pathway is IL-17 signaling, which has been shown to promote the development of tumors in multiple organs, and confer therapy resistance to tumors in the colon and other organs<sup>23–30</sup>. Interestingly, blockade of IL-17 signaling by genetic ablation of its cognate receptor resulted in increased expression of immune checkpoint markers such as PD-1 and CTLA-4<sup>31</sup>. On the other hand, treatment with anti-CTLA-4 antibody led to increased expression of pro-tumor IL-17, indicating that IL-17 and immune checkpoint signaling are mutually inhibitory. Given their common roles in limiting anti-cancer immunity and promoting therapy resistance, simultaneous inhibition of IL-17 and immune checkpoints may generate synergistic anti-cancer efficacy in cancer treatment.

IL-12 is one of the most potent antitumor cytokines evaluated to date as a potential immunotherapy for cancer. This cytokine is chiefly responsible for the induction and enhancement of cell-mediated immunity. As a heterodimeric cytokine, comprising 35 kD and 450 kD subunits, IL-12 potently stimulates Th1-armed immunity<sup>32,33</sup>. Among its diverse functions, IL-12 has been shown to: (i) induce Th1 cell differentiation; (ii) increase activation and cytotoxic capacities of T and NK cells; and (iii) inhibit or reprogram immunosuppressive cells, such as tumor-associated macrophages (TAMs) and myeloid-derived suppressor cells (MDSCs)<sup>34–38</sup>. IL-12 also induces the production of large amounts of IFN- $\gamma$ , which itself is cytostatic/cytotoxic<sup>39,40</sup>, anti-angiogenic<sup>41,42</sup>, and can upregulate MHC I and II expression on tumor cells for enhanced recognition and lysis<sup>43</sup>. IL-12 has shown remarkable antitumor effects against a range of malignancies in preclinical studies<sup>44–47</sup>. These effects are largely dependent on CD8<sup>+</sup> T cells, NK cells, and NK T cells<sup>47–49</sup>.

However, the much-anticipated clinical translation of IL-12-based immunotherapies suffered a tremendous setback a couple of decades ago due to disappointing antitumor responses and severe clinical toxicities associated with systemic IL-12 injections. Since the ideal targets of IL-12 immunotherapy are the immune cells within the tumor and nearby lymph nodes, including activated but exhausted T cells, NK cells, TAMs, and MDSCs<sup>50</sup>, maximizing the amount of IL-12 that reaches the tumor seems critical for a

robust antitumor response. Moreover, localized delivery strategies are capable of enhancing IL-12 concentrations in the TME by one or more orders of magnitude<sup>31,51–53</sup>. Despite these challenges, IL-12's pleiotropic activity, such as its ability to engage multiple effector mechanisms and reverse tumor-induced immunosuppression still presents an attractive target for immunotherapy. As exemplified by the current clinical trial landscape and by several promising preclinical studies with localized IL-12, combination approaches appear to be most effective for accelerating clinical impact. Oncolytic virus therapy, immune checkpoint inhibitors (ICI), and other cytokines (such as IL-17) are ideal candidates for combination with IL-12. For example, IL-12 expressed in alpha-virus induces PD-L1 expression on cancer cells when combined with PD-1/PD-L1 blockade, significantly enhanced long term survival<sup>54</sup>.

In this study, we tested the hypothesis that arming oncolytic VLV with a combination of IL-12, shRNA for PD-L1 and a dominant negative IL-17 receptor A (dnIL-17RA) transgenes would generate an effective therapeutic agent needed to regress tumor growth. Herein, we demonstrate the utility of deploying VLV to deliver multiple immune modulators to tumors, and we show that the combination therapy not only regressed tumor growth but also prolonged the survival of mice in syngeneic ectopic model of colorectal cancer and hepatocellular carcinoma. Intriguingly, this combination virotherapy was sufficient to prevent tumor recurrence in mice. Thus, the ability of CARG-2020 to prevent tumor recurrence in mice and to extend their survival makes it a promising candidate for use in human cancer immunotherapy.

## 2. Materials and methods

### 2.1. Generation of VLV-based constructs

In order to generate VLV-IL-12 and CARG-2020 constructs, the vector VLV dp, which has previously been described<sup>10</sup>, was linearized by AscI/SbfI restriction digestion. A purified DNA fragment encompassing VSV glycoprotein (G) gene of the New Jersey (NJ) serotype was ligated by compatible ends. The resulting construct of VLV dp-VSV-G<sup>NJ</sup> was next digested with BamHI/PacI and served as a vector for inserting transgenes of interest. To clone the VLV-IL-12 construct, mouse versions of the IL-12p40 (NCBI Accession # NP\_001290173.1) and IL-12p35 (Accession # NP\_001152896.2) subunits were commercially synthesized (Thermo Fisher Scientific, MA, USA) fused together by PCR using an elastin linker. The synthetic DNA was then PCR-amplified using a pair of primers that contain flanking BamHI and PacI cloning sites. Both PCR fragments were amplified with Q5<sup>®</sup> high-fidelity DNA polymerase, purified from the gel, and infused into VLV dp-VSV-G<sup>NJ</sup> vector. In order to generate the CARG-2020 construct containing three transgenes namely IL-12, IL-17RA (Accession # NP\_032385.1) and shRNA target sequences derived from PD-L1 (Accession # NM\_021893.3), the full-length IL-12 fragment (encompassing both fused subunits), and an IL-17RA extracellular domain (ECD) containing a 3' HA-tag and PD-L1-shRNA synthetic gene fragment incorporating three shRNA concatemers (Sh-1: 5'-ATTGCTGGCATTATATTCAC-3'; Sh-2: 5'-GCTGAAAGTCAATGCCCC ATA-3' and Sh-3: 5'-CTGGACAAACAGTGACCACCA-3') were amplified and infused into VLV dp-VSV-G<sup>NJ</sup> between BamHI/PacI cloning sites. To clone GFP, IL-17RA-Ant, and PD-L1 shRNA separately

into VLV vector, inserts were amplified and cloned in VLV dp-VSV-G<sup>NJ</sup>. All primers to amplify DNA fragments were designed according to NEBuilder instruction and infused into VLV dp-VSV-G<sup>NJ</sup> vector using NEB HiFi DNA Assembly Kit (E5520S). The recombinant clones were screened for positive inserts by DNA restriction digestion. The final positive constructs were further confirmed by DNA sequencing (GENEWIZ, NJ, USA).

### 2.2. VLV production

To produce VLV stocks, BHK-21 cells were cultured in Dulbecco's modified Eagle medium supplemented with 5% fetal bovine serum (FBS). VLVs were produced by transfecting BHK-21 cells with the VLV plasmid DNA followed by collection of the master VLV stock. Propagation of the working stocks was performed by a single passage of the master stock in BHK-21 cells cultured in Opti-MEM<sup>™</sup> Reduced Serum Medium (Thermo Fisher, Waltham, MA, USA). Working stocks were concentrated using MacroSep<sup>®</sup> Advance 100K MWCO (Pall Laboratories, Port Washington, NY, USA) and VLVs were routinely titered using serial dilutions and a standard 2-d plaque assay on BHK-21 (ATCC CCL 10) cell monolayers as previously described<sup>9</sup>. VLV plaques were counted using a dissecting microscope.

### 2.3. In vitro PD-L1 knock-down

To examine the *in vitro* PD-L1 downregulation by CARG-2020, MC38 cells were stimulated with 20 ng/mL mouse IFN- $\gamma$  and at the same time infected with two multiplicity of infection (MOI) of the indicated VLVs. After 26 h of stimulation/infection, cells were lifted and stained for PD-L1 (cat#124308, BioLegend), and analyzed for the percentage of PD-L1-positive and -negative cells by flow cytometry. For data analysis, we used GraphPad Prism software, version 9 (GraphPad Software, San Diego, CA). BHK21 cells stably expressing PD-L1 transgene were infected with PD-L1 shRNA VLV at 1 MOI infection. Cells collected by scraping and analyzed by Western blot probed with anti-PD-L1 (Bio X cell # BE0101), and anti- $\beta$ -actin (Santa Cruz Biotechnology) antibodies. PD-L1 band densities were analyzed and normalized with actin loading control.

### 2.4. Tumor immunotherapy models

MC38 and BNL-T3 cells were cultured in Dulbecco's modified Eagle medium supplemented with 10% FBS, penicillin, and streptomycin. Cultured cells were digested with trypsin, suspended in PBS, and injected subcutaneously into the flanks of 2–3 months old C57BL/6J (for MC38 cells) or BALB/c (for BNL-T3) mice. Equal numbers of male and female mice were used for the tests, and mice were assigned randomly into different treatment groups. Tumor length and width were measured every two days with a caliper. Tumor volume was calculated as  $V = (\text{Length} \times \text{Width}^2)/2$ . VLVs were given intratumorally at a dose of  $5 \times 10^7$  PFU per injection at indicated time points. Mice were sacrificed at indicated time points for biochemical and flow cytometry analyses, or continuously followed for tumor growth until their tumor volume reached 3 cm<sup>3</sup>, at which point they were sacrificed. Both male and female mice were used for all experiments. All mice were kept at a specific-pathogen-free facility, and all mouse experiments were approved by the Institutional Animal Care and Use Committee at UConn Health.

### 2.5. Flow cytometry

Tumors were dissected from mice, minced with scissors, and digested with 1 mg/kg collagenase IV (Sigma Aldrich) for 20 min. Dissociated tumor cells were filtered with a 70  $\mu$ m cell sieve and stained with Live/Dead fixable exclusion dye (Tonbo Bioscience, Cat #13-0868), followed by fluorochrome-conjugated antibodies in PBS with 2% FBS and 1 mmol/L EDTA. Anti-CD3 (Cat # 100206), anti-CD4 (Cat #100536), anti-CD45 (Cat # 103138), and anti-IFN- $\gamma$  (Cat #505806) antibodies were from Biolegend. Anti-Foxp3 antibody (Cat # 11-5773-82) was from eBioscience. Anti-CD8 $\alpha$  antibody (Cat # 558106) was from BD Bioscience. For intracellular cytokine staining, cells were stimulated with a Cell Stimulation Cocktail (eBioscience, Cat #00-4975-93) for 4 h, followed with fixation and staining with Foxp3/transcription factor staining buffer set (eBioscience, Cat #00-5523-00). Flow cytometry analyses were performed on a BD LSRII flow cytometer. Data were analyzed with FlowJo software (FlowJo, LLC).

### 2.6. qRT-PCR

Tissues from primary tumors were harvested for RNA extraction (Qiagen). DNA contamination in the samples was removed with DNA-free Kit (AM1906). cDNA was synthesized using Bio-Rad iScript<sup>TM</sup> Advanced cDNA Synthesis Kit (1725037). qPCR was performed to quantify mRNAs of indicated genes on a BioRad CFX96 real-time PCR machine using SSO advanced SYBRGreen mix (1725271). GeneQuery mouse qPCR array 96-well plate kit (GQM-PD1#MGK121) was used to amplify and measure target genes. The GEOMEAN expression of 5 housekeeping genes ( $\beta$ -actin, B2m, Gapdh, Gusb, and Hprt) were measured as endogenous controls. Along with the kit primer set, other primer sequences were used (Supporting Information Table S1) to detect other mRNA transcripts. Gene expression was quantified by the comparative  $\Delta\Delta$ CT method. To perform all calculations, we used GraphPad Prism software, version 9 (GraphPad Software, San Diego, CA). To determine the difference between the experimental groups, we applied 2-way ANOVA for analyses between the groups with Sidak's multiple comparison test.

### 2.7. Statistical analysis

Statistical analysis was performed with GraphPad Prism version 9 (GraphPad Software, San Diego, USA) unless stated otherwise. A *P* value below 0.05 was considered significant, except for survival curve comparisons where *P* value thresholds were manually corrected for multiple comparisons. Longitudinal data were analyzed by two-way ANOVA or a mixed effects analysis where appropriate and referred to as two-way ANOVA type. In case three or more groups were compared, Tukey's or Dunnett's post testing was performed, depending on the number of pairwise comparisons. One-dimensional data were analyzed by unpaired, two-sided Mann–Whitney test and Kruskal–Wallis test when two and three or more groups were compared, respectively. Survival data were analyzed by pairwise curve comparisons using Gehan'–Breslow–Wilcoxon test followed by manual Bonferroni *P* value adjustments correcting for multiple comparisons. Unless stated otherwise, *n* is the number of biological replicates (individual mice, organs, or human donor PBMC samples).

### 2.8. Data access

The data generated in this study are available upon request from the corresponding author.

## 3. Results

### 3.1. IL-12, IL-17 and PD-L1 shRNA affect tumor growth

The VLV platform is a hybrid viral system comprising DNA sequences encoding Semliki Forest Virus (SFV) replicase complex (SFV nsp1-4) and vesicular stomatitis virus glycoprotein (VSV-G) allowing expression of antigens as a payload<sup>7–9</sup>. To determine the suitability of the VLV platform for expression of immunomodulatory payloads, we generated single-chain IL-12, dnIL-17RA, and PD-L1 shRNA, cloned them separately into the VLV vector, and examined their expression by Western blot analysis (Fig. 1a and b). A GFP-expressing VLV construct was used as a control (Fig. 1a and b). VLV-IL-12 delivers a single chain IL-12 that has been shown to promote Th1 differentiation<sup>55</sup> (Fig. 1b). VLV-IL-17RA-Ant produces a secreted form of the extracellular domain of IL-17RA, which is known to bind to IL-17, but is insufficient to relay its signaling<sup>56</sup>, thus acting as a dominant negative form for the receptor (Fig. 1b). VLV-PD-L1-shRNA delivers three shRNAs targeting PD-L1 and thus downregulates the expression of this immune checkpoint ligand (Fig. 1b). We tested each of the individual VLV constructs in the MC38 model of syngeneic colon cancer in mice<sup>57</sup>. Intratumoral injection of VLV-IL-12 to subcutaneously grafted and established MC38 tumors markedly arrested tumor growth and resulted in tumor shrinkage (Fig. 1c). In comparison, VLV-IL-17RA-Ant and VLV-PD-L1-shRNA exhibited partial tumor growth inhibition that was statistically significant from the VLV-GFP used as a vector control (Fig. 1c). These results indicate that each of the IL-12, IL-17RA-Ant, and PD-L1 shRNA payload functions independently, and suppresses colon tumor growth to a different degree.

### 3.2. Intralesional injection of multivalent CARG-2020 vector results in tumor retraction and eradication

To explore if the simultaneous delivery of all three payloads (IL-12, IL-17RA-Ant, and PD-L1 shRNA) from a single VLV vector will result in superior cancer treatment efficacy, we generated a construct that carries IL-12, IL-17RA-Ant, and PD-L1 shRNAs in tandem (Fig. 2a). We designated the new construct as CARG-2020. When used to infect MC38 colon cancer cells, CARG-2020 delivers secreted IL-12 and IL-17RA-Ant (Fig. 2b), and downregulates the expression of PD-L1 (Fig. 2c).

To test the efficacy of CARG-2020, we compared this trivalent agent with VLV-IL-12, which exhibited the strongest therapeutic efficacy among the three monovalent VLVs (Fig. 1c). MC38 cells were inoculated subcutaneously into the flanks of C57/BL6 mice. Fifteen days after tumor inoculation, subcutaneous MC38 tumors reached average sizes around 600 mm<sup>3</sup>. VLVs carrying GFP, IL-12 (VLV-IL-12), or trivalent payloads (CARG-2020) were injected intratumorally on Days 15, 17, and 21 (Fig. 3a). Treatment of MC38 tumors with VLV-IL-12 and CARG-2020 showed similar effect on tumor regression, and resulted in tumor shrinkage within 10 days after final dosage (Fig. 3b and c). To observe the long-term effect of VLV-based immunotherapy against MC38 tumors,



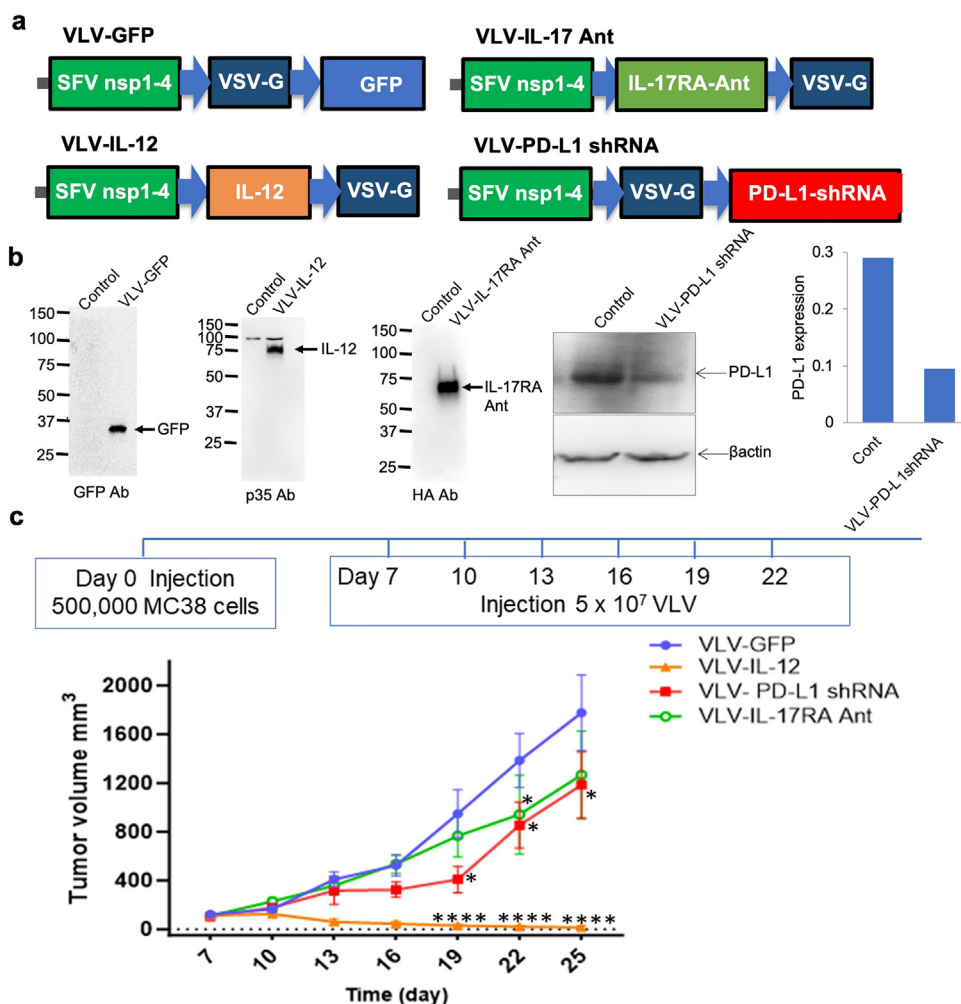


**Figure 1** Armed VLV RNA replicon platform promotes tumor regression. (a) Design of VLV constructs comprised of SFV 1-4 non-structural protein (nsp) and VSV-G structural glycoprotein. Transgenes encoding GFP, a single chain IL-12, the extracellular domain (ECD) of IL-17RA (IL-17RA Antagonist), and shRNAs against PD-L1 were cloned into VLV vector backbone to generate respective payload VLV constructs. (b) Each payload of VLV was used to infect BHK-21 cells at one MOI. 24 h later, an aliquot of cell culture lysates was analyzed by Western blotting for GFP (left, using anti GFP antibody), for IL-12 (middle, using anti-IL-12p35 antibody) and IL-17RA antagonist (right, using HA antibody against HA-tagged IL-17RA ECD) for transgene expression. BHK-21 cells that stably express PD-L1 were infected with 1 MOI VLV PD-L1 shRNA. Cells were lysed and blotted against anti-PD-L1 and anti- $\beta$ -actin antibodies. Relative expression of PD-L1 compared to  $\beta$ -actin was quantified in the right panel. (c)  $5 \times 10^5$  MC38 cells were grafted subcutaneously to the flank of C57BL/6J mice. At indicated dates,  $5 \times 10^7$  pfu indicated VLV agents were injected intratumorally. Tumor sizes were measured every three days, and average tumor sizes of each group were shown. Error bars denote SEM. \* $P < 0.05$ , \*\* $P < 0.01$ , \*\*\*\* $P < 0.0001$ .

we followed the tumor-bearing mice for 76 days from tumor inoculation. Treatment with VLV-IL-12 suppressed tumor growth for 2 weeks, but from Day 33 onwards, and in 5 out of 7 mice we observed tumor regrowth (Fig. 3b and c). On the other hand, CARG-2020 treatment resulted in complete eradication of MC38 tumors in 6 out of 7 mice (Fig. 3b and c), and no tumor recurrence was observed even on Day 75 in 5 animals. To fully inhibit tumor growth in the one mouse with recurrent tumor, we administered two additional doses of CARG-2020 on Days 50 and 54. This additional treatment resulted in complete tumor eradication (Fig. 3b and c). Survival analysis showed significantly longer overall survival in mice treated with CARG-2020 compared to mice treated with VLV-IL-12 or VLV-GFP (Fig. 3d). We did not observe any treatment-related deaths in all groups of animals,

demonstrating the safety of CARG-2020 in particular and the VLV platform in general when given intratumorally. Overall, our results show that CARG-2020 is superior in achieving complete eradication of MC38 tumors and maintaining tumor-free survival of experimental animals (Fig. 3b and c) compared to VLV-IL-12 that lacks the capability to inhibit IL-17 and PD-1 signaling pathways.

### 3.3. CARG-2020 treatment protects with tumor re-challenge

To test if treatment of CARG-2020 confers long-term immune memory to cancer, we re-challenged VLV-IL-12 and CARG-2020-treated mice with MC38 tumor graft, 4 months and 7 months after initial tumor graft. None of the 5 mice in CARG-2020-treated

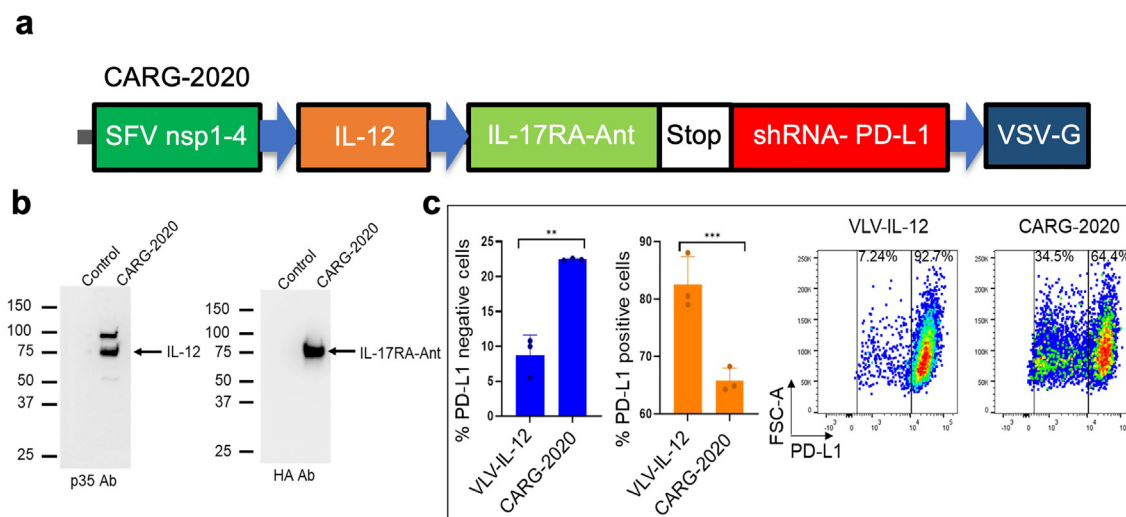


**Figure 2** Design, cloning and expression of CARG-2020 VLV. (a) Design of CARG-2020, a VLV construct with payload comprised of a single chain IL-12, extracellular region of IL-17RA serving as an antagonist for the IL-17 pathway (IL-17RA Ant), and shRNAs against PD-L1. (b) CARG-2020 was used to infect BHK-21 cells at one MOI. 24 h later, an aliquot of cell culture supernatant was analyzed by Western blotting for IL-12 (left, using anti-IL-12p35 antibody) and IL-17RA antagonist (right, using HA antibody against HA-tagged IL-17RA ECD) transgenes expression. (c) MC38 cells were stimulated with 20 ng/mL mouse IFN- $\gamma$  and infected with 2 MOI of VLV-IL-12 or CARG-2020. After 26 h of infection and stimulation, cells were lifted and stained for PD-L1, followed by flow-cytometry analysis. The left panel graph shows the percentages of PD-L1-positive and -negative MC38 cells. Representative FACS dot plots are shown on the right.  $**P < 0.01$ ,  $***P < 0.001$ .

group showed any signs of tumor growth during these two rounds of re-challenge (Fig. 3e). However, only 3 animals in VLV-IL-12 treated group showed no tumor growth (Fig. 3e). These data further confirm a long-term immune memory against the same type of tumors in both CARG-2020 and VLV-IL-12-treated groups.

### 3.4. Biodistribution and oncolytic activity of hCARG-2020

As next steps in the development of CARG-2020 for immunotherapy of cancer in humans, we generated a “humanized” CARG-2020 (hCARG-2020) version by replacing the payloads with human sequences of single chain IL-12, IL-17RA-Ant, and PD-L1 shRNA (Supporting Information Fig. S1a). We aim to use the hCARG-2020 for our clinical investigation in future. We subsequently injected  $5 \times 10^7$  pfu of hCARG-2020 to established MC38 tumors, and assayed the distribution of VLV genes and payloads in different organs in mice. mRNAs of human IL-12 and IL-17RA-Ant, as well as VSV-G, were largely restricted to the tumor (Fig. S1). Low levels of transgenes were found in the blood and the lung 24 h after the injection, and by 48 h, all tissues other than the tumor were devoid of viral genes or payloads (Fig. S1b–d). These results suggest that distribution of CARG-2020 is predominantly restricted to the tumor.

### 3.5. CARG-2020 treatment results in abscopal anti-tumor effects

Oncolytic viruses have been shown to be effective when injected intratumorally, and may elicit systemic immunity and exert therapeutic effects against distal tumors<sup>3</sup>. Next, to examine whether localized activation of immune responses by CARG-2020 affects systemic disease, we conducted a bilateral MC38 model in which mice had subcutaneous MC38 tumors inoculated into both flanks.

To test if CARG-2020 induces therapeutic immune memory against distal tumors, we first inoculated MC38 tumor cells into the right flanks of mice. The resulting tumors are hereon referred to as “primary tumors.” Four days later, we inoculated MC38 cells into the left flanks of the same mice to allow the growth of distal, non-treated tumors (secondary tumors). We started intralesional injection of CARG-2020 and VLV-GFP into primary tumors on Day 14 (Fig. 4a). Consistent with our previous finding, treatment of primary MC38 tumors by CARG-2020 quickly stopped their growth, leading to tumor shrinkage and eradication (Fig. 4b). More importantly, treatment of the primary tumors by CARG-2020 also resulted in significantly delayed growth of the secondary tumors compared to VLV-GFP treatment (Fig. 4c). These data demonstrate abscopal effects of CARG-2020 on untreated distal tumors from immunological memory generated by treatment. Treatment with CARG-2020 did not result in observable distress in mice, or significant reduction in bodyweight (Fig. 4d). As a result of the suppression in primary tumor, and delayed secondary tumor growth, CARG-2020 treated mice survived significantly longer compared to control vector treated groups (Fig. 4e). The disappearance of the tumors that had been directly injected with CARG-2020 VLV and the prolonged suppression of noninjected contralateral tumors (Fig. 4b and c), supports the potential efficacy of this viral therapy against distant metastatic disease.

### 3.6. CARG-2020 modulates IL-12, IL-17R, and PD-L1 signaling in tumors

To further understand the difference between VLV-IL-12 and CARG-2020 treatments on the tumor microenvironment immunity at both molecular and cellular levels, we employed the MC38 model of colon cancer on mice<sup>57</sup>. C57BL/6J mice of 2–3 months of age were inoculated with  $5 \times 10^5$  MC38 cells subcutaneously to initiate tumor growth. VLV-IL-12, CARG-2020, and GFP-expressing VLV as controls, were injected intratumorally on

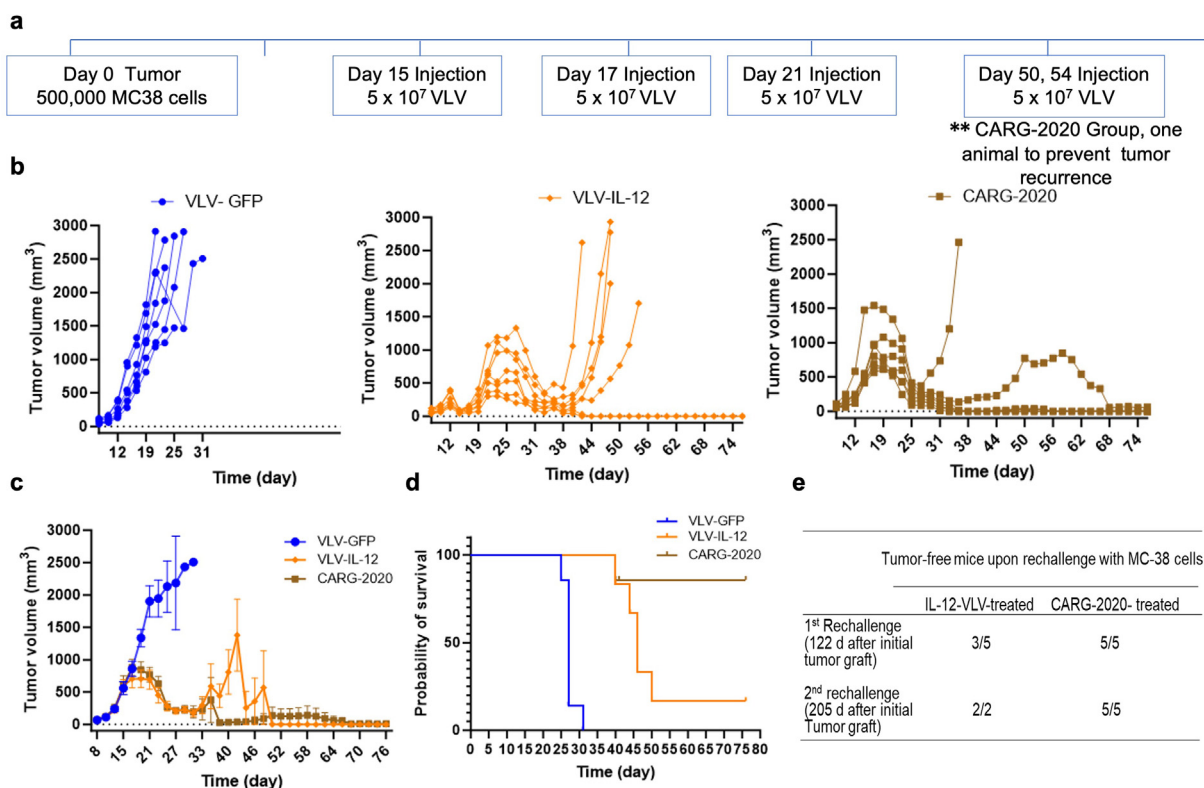


**Figure 3** CARG-2020 effectively eradicates MC38 tumors when given intraslesionally and prolongs survival. (a)  $5 \times 10^5$  MC38 cells were injected subcutaneously to C57BL/6J mice on Day 0. On Days 15, 17, and 21, tumors were injected with VLV carrying GFP (VLV-GFP), VLV-IL-12, or CARG-2020 at a dose of  $5 \times 10^7$  pfu. Tumor lengths and widths were measured with a caliper every 2 days, and tumor volumes were calculated as  $(\text{Length} \times \text{Width}^2)/2$ . (b) Tumor volume of individual mice treated with indicated VLV agents over time. Mouse #2 in the CARG-2020 group received additional treatment on Days 50 and 54 at the same dose as indicated by \*\*. (c) Average tumor volume of mice treated with indicated VLV agents over time.  $N = 8$  for VLV-GFP,  $n = 7$  for both VLV-IL-12 and CARG-2020. Data represent mean  $\pm$  SEM. (d) Percentage of mice surviving during the treatment. No treatment-related deaths were observed. Mice were sacrificed when their tumor volume reached or exceeded  $3 \text{ cm}^3$  on the day of measurement. (e) MC38 tumor-bearing mice were treated with multiple doses of VLV-IL-12 and CARG-2020 to achieve tumor eradication. At 122 days after initial tumor graft (2.5 months after the last dose of VLV injection), mice were challenged with subcutaneous injection of  $5 \times 10^5$  MC38 cells, and tumor growth was followed. The number of mice that remained tumor free for at least one month following rechallenge are shown. Similarly, 12 weeks later, a second round of tumor rechallenge was performed on surviving mice, and tumor-free ratio is also shown here.

Days 14 and 16 after tumor inoculation, and mice were sacrificed on Day 20 for flow cytometry and q-RT-PCR analyses (Fig. 5a). Treatment with VLV-IL-12 and CARG-2020 induced strong activation of Th1 cells in tumors, signified by the increased production of IFN- $\gamma$  by CD4 T cells (Fig. 5b–d). The proportions of CD8<sup>+</sup> T cells that express IFN- $\gamma$  were also much higher in VLV-IL-12- and CARG-2020-treated tumors, suggesting a potent activation of Th1-armed immunity in the primary tumor (Fig. 5b–d). In addition to local immune activation, VLV-IL-12 and CARG-2020 also induced the activation of Th1 cells and CD8<sup>+</sup> T cells in the spleen, thus suggesting a systemic immune response (Fig. 5b–d). Additionally, the number of regulatory T cells (Tregs; Foxp3<sup>+</sup>) significantly decreased in VLV-IL-12- and CARG-2020-treated tumors (Fig. 5b–d). Since Tregs have been shown to promote tumor evasion and have become the target of cancer immunotherapy<sup>58,59</sup>, the reduced proportion of Tregs and increased Th1 cells among CD4<sup>+</sup> T cells in the tumor predicts favorable treatment outcomes for CARG-2020 and VLV-IL-12.

In order to better understand possible mechanism that prolongs tumor recurrence particularly with CARG-2020 treatment, we

undertook gene profiling of tumors between CARG-2020 and VLV-IL-12 animal groups. Expression of CXCL1/2 (IL-17 targets) decreased in CARG-2020 groups, confirming that the extracellular domain of IL-17A receptor inhibits IL-17 signaling. Delivery of IL-12 by VLV-IL-12 resulted in increased expression of PD-L1 and CXCL1 family chemokines (Fig. 5e). The overexpression of inhibitory receptors such as PD-L1 may lead to T cell exhaustion in the tumor microenvironment. Since they are key players in cancer-related inflammation, increasing evidence suggests that chemokines produced by tumor cells are the mediators of metastasis, and downregulation of CXCL1 and CXCL2 is associated with a marked inhibition of metastasis-promoting genes. The ability of CARG-2020 to downregulate PD-L1 expression in the TME by preventing immune cell exhaustion (Fig. 5e), coupled with the marked attenuation of CXCL1 and CXCL2 by CARG-2020 treatment portend well for a favorable response in the clinic. Gene profiling data showed expression of gene signatures for T cell infiltration (Fig. 6a and Supporting Information Fig. S2a), co-stimulation (Fig. 6b and Fig. S2b), and expression of MHC II in tumors (Fig. S2c). VLV-IL-12-treated tumors showed

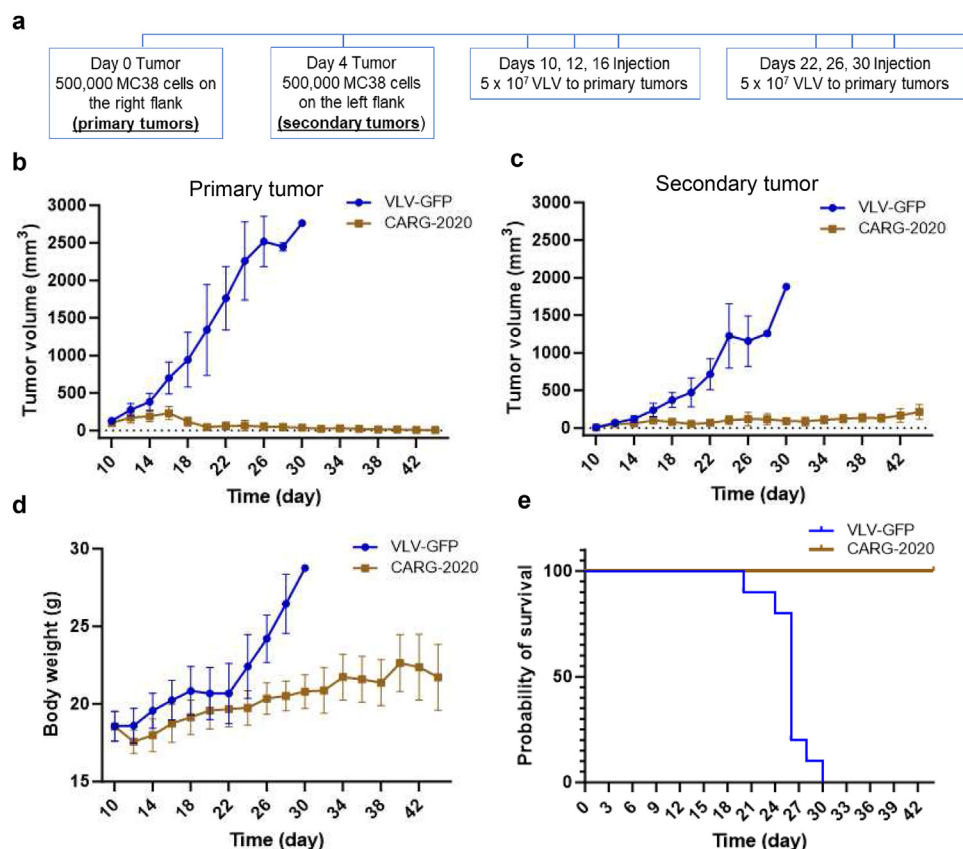


**Figure 4** Treatment with CARG-2020 mounts therapeutic effect against distant tumors. (a)  $5 \times 10^5$  MC38 cells were injected subcutaneously to the right flank of C57BL/6J mice on Day 0 (primary tumors) and on Day 6 (secondary tumors). On indicated days, primary tumors were injected with VLV carrying GFP (VLV-GFP) or CARG-2020 at a dose of  $5 \times 10^7$  pfu. (b, c) Volumes of primary (b, treated) and secondary (c, untreated) tumors were measured and calculated as previously described.  $N = 10$ . Data represent means  $\pm$  SEM. for average tumor volumes. (d) Average body weights of mice under indicated treatment. (e) Percentage of mice surviving at indicated time points.

upregulation of signatures of immune exhaustion (Fig. 6c and Supporting Information Fig. S3a), immunosuppressive network that promote tumor growth (Fig. 6d), and cancer-promoting inflammation (Fig. 6e and Fig. S3b). However, CARG-2020 therapy restores these signatures to normal levels in the TME, plausibly through its inhibition of IL-17 and PD-1 pathways (Fig. 5d, e and Fig. S3a and S3b). Treatment with CARG-2020 also reduced expression of cancer stem cell markers (Fig. 6e and Fig. S3c) and signaling components of oncogenic pathways (Fig. 6c and Fig. S3d). Taken together, when compared to the delivery of IL-12 alone, our multivalent approach using CARG-2020 to modulate IL-12, IL-17, and PD-L1 signaling achieved superior tumor immune modulation by downregulating tumor promoting inflammation, immune suppression, T cell exhaustion, and cancer stemness/oncogenic signaling (Fig. 6f). These properties are consistent with our observation of enhanced tumoricidal effect of CARG-2020 against MC38 tumors and the suppression of tumor recurrence by CARG-2020.

### 3.7. CARG-2020 is superior to PD-1 blockade in treatment of MC38 tumors

Immune checkpoint inhibitors, such as PD-1 blockade, have seen great success in cancer treatment. To compare the effect of PD-1 blockade with CARG-2020, which also includes PD-L1 blocking

moiety, we treated MC38 tumor bearing mice with PD-1 blocking antibody or by intratumoral injection of CARG-2020. Each mouse was grafted with two tumors, 4 days apart, and received either i.p. injection of PD-1 blocking antibody, or i.t. injection of CARG-2020 to the primary tumor (Fig. 7a). Isotype antibody was used as a control for anti-PD-1. Interestingly, treatment with PD-1 antibody had no obvious effects on the larger primary tumors, but slowed down the growth of smaller secondary tumors in mice (Fig. 7b and c). In contrast, CARG-2020 displayed significantly better efficacy against both the large primary tumors that received i.t. injection, and distant, smaller secondary tumors that did not receive the agent (Fig. 7b and c). No weight loss was observed during the experiments (Fig. 7d) and increased survival was associated with CARG-2020 treatment (Fig. 7e). It is plausible that CARG-2020 harboring the three immunomodulators generated a strong immunological memory against tumor specific neoantigens released by VLV-mediated oncolytic activity. These results suggest that CARG-2020 is superior to PD-1 blockade for the treatment of primary as well as distant noninjected secondary tumors. Since checkpoint inhibitors are effective when combined, they also carry the risk of severe cumulative adverse effects. The ability to combine therapies in CARG-2020 using a genetic approach that delivers IL-12, IL-17RA antagonist, and PD-L1 shRNA locally into tumors obviates the need to combine antibodies with concomitant safety concerns.



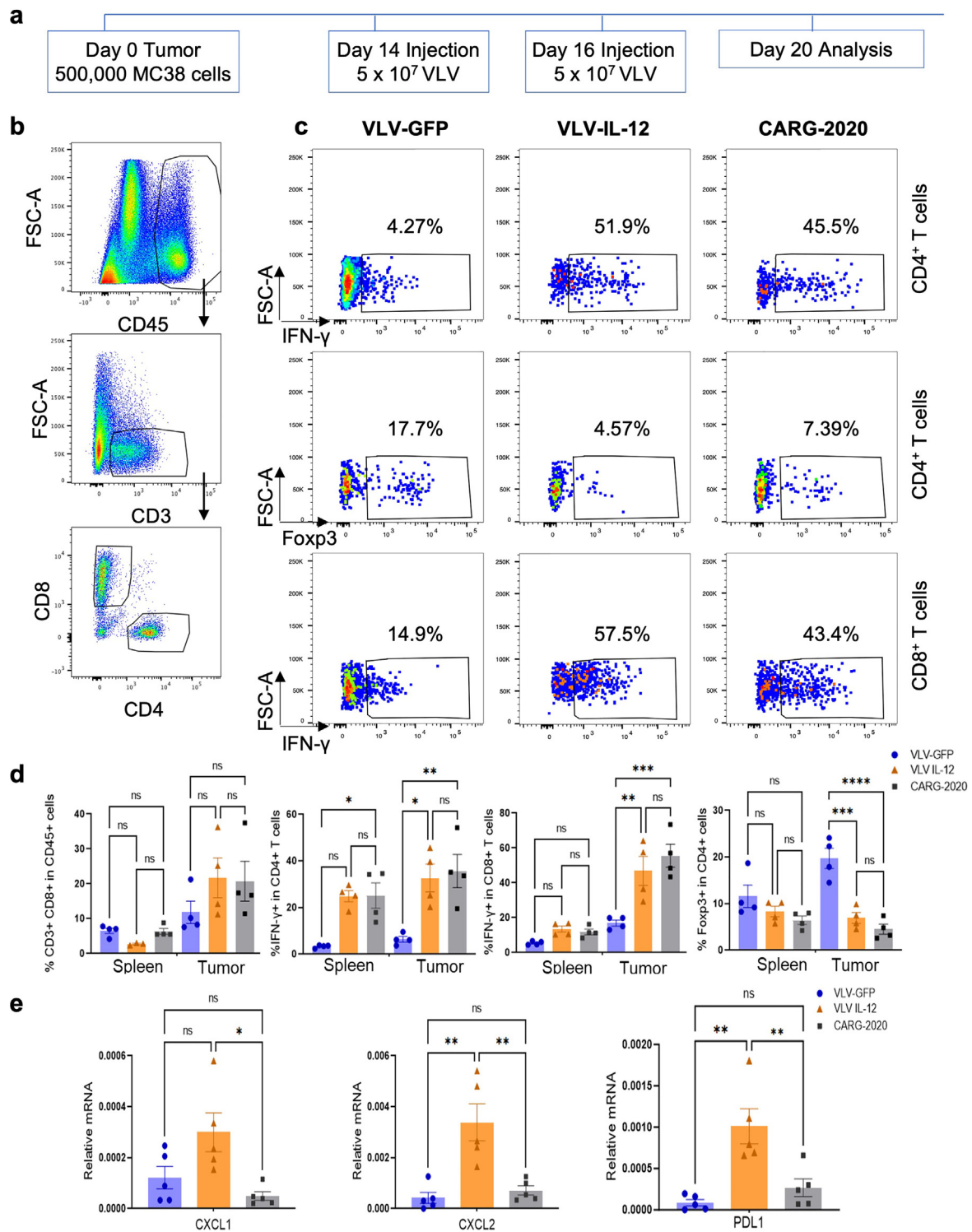


**Figure 5** CARG-2020 activates Th1-armed immunity, and inhibits expression of CXCL1, CXCL2 and PD-L1. (a)  $5 \times 10^5$  MC38 cells were injected subcutaneously to C57BL/6J mice on Day 0. On Day 14 and 16,  $5 \times 10^7$  VLV particles were injected intraslesionally. Mice were sacrificed on Day 20, and their tumors and spleens were harvested for analyses. (b–d) Isolated single cells from spleens and tumors were stimulated for 6 h *in vitro* with PMA/ionomycin in the presence of Brefeldin A and monensin. Cells were then stained with fluorescence-labeled antibodies and analyzed by flow cytometry. (b) Representative gating charts for isolated live tumor cells. All data shown in (b) were gated on live cell/CD45<sup>+</sup> population. (c) Representative gating charts for tumor-infiltrating CD4<sup>+</sup> and CD8<sup>+</sup> T cells stained with antibodies against IFN- $\gamma$  and Fcpx3. (d) Percentages of indicated cell populations in the spleens and tumors of VLV-GFP, VLV-IL-12, or CARG-2020 treated mice.  $N = 5$  for VLV-GFP;  $n = 5$  for VLV-IL-12; and  $n = 5$  for CARG-2020. Data represent means  $\pm$  SEM. \* $P < 0.05$  in Student's *t* test. (e): Tumors treated with indicated agents were harvested for mRNA isolation and q-PCR analysis.  $N = 4$  for VLV-GFP;  $n = 8$  for VLV-IL-12; and  $n = 8$  for CARG-2020. Data represent means  $\pm$  SEM. \* $P < 0.05$ , \*\* $P < 0.01$ , \*\*\* $P < 0.001$ .

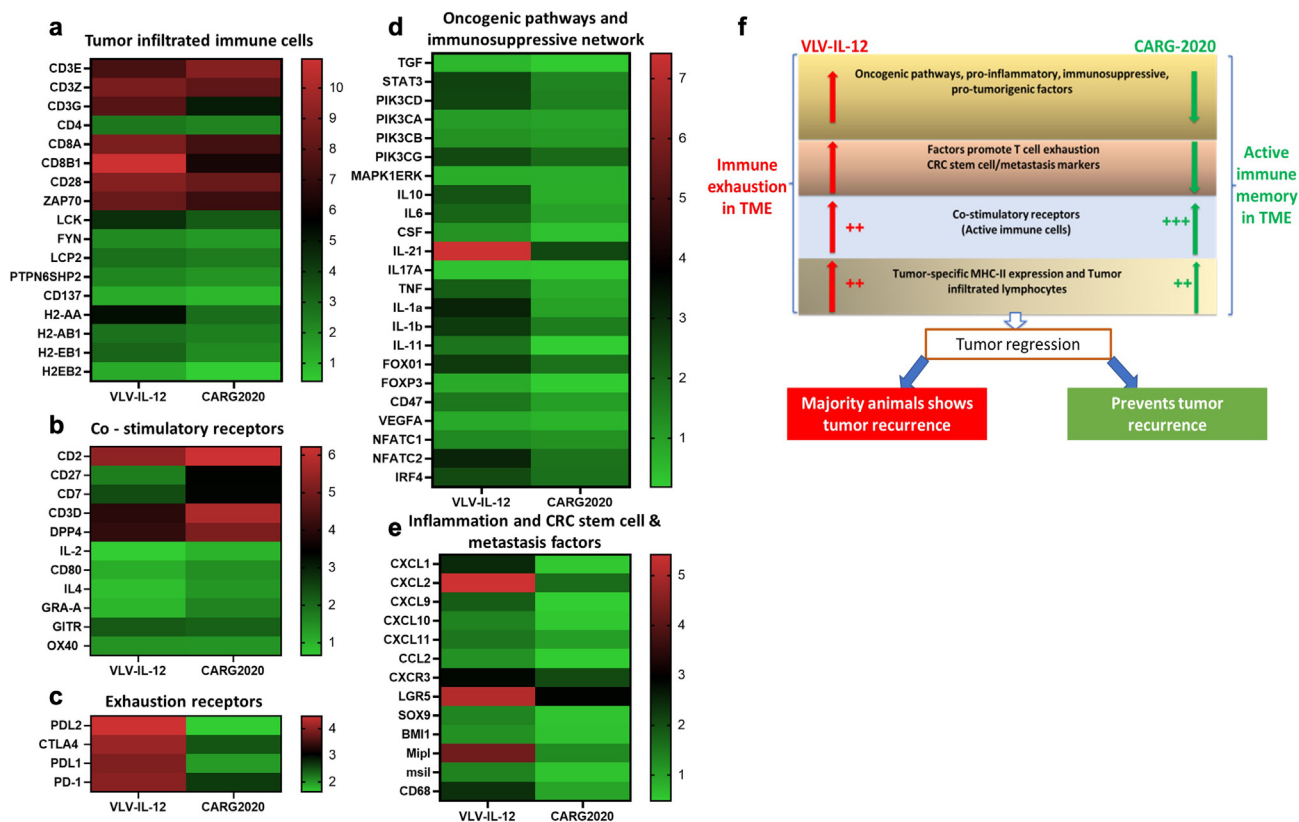


**Figure 6** Expression profile of immune-related related pathways in the tumor microenvironment of IL-12 and CARG-2020 VLV- treated mice. MC38 tumors were treated as shown in Fig. 2a. Tumor tissues were harvested for mRNA extraction, and expression of indicated genes were analyzed by q-RT-PCR. (a–e) Heatmaps were assembled from RT-qPCR analysis of mRNA levels in VLV-IL-12, and VLV-CARG-2020-treated tumor samples. Heat maps were generated using GraphPad Prism software, version 9 (GraphPad Software, San Diego, CA). Values are geometric means of the fold changes compared to VLV-GFP in each group ( $n = 8$  for VLV-IL-12 and CARG-2020). Color intensity is proportional to levels of gene expression, with green annotating lower expression, and red annotating higher expression. (f) Schematic representation of the immune- and cancer-modulating effects of CARG-2020 compared to VLV-IL-12. Oncogenic pathways, pro-tumorigenic and immunosuppressive networks are active in IL-12 VLV-treated tumors. This led to immune cell exhaustion in the tumor microenvironment. Overexpression of exhaustion markers in IL-12 VLV-treated tumors most likely turned the initially active immune environment in the two therapies into exhaustion phase for IL-12 and thereby allows tumors to recur. Downregulation of CRC stem cell and metastasis markers by CARG-2020 further supports the notion of preventing tumor recurrence.

### 3.8. CARG-2020 is effective in the treatment of liver cancer

To confirm the efficacy of CARG-2020 in treating other tumors, we performed a similar study using the BNL-T3 model of liver cancer<sup>60</sup>. Treatment of subcutaneously grown BNL-T3 tumors with three doses of CARG-2020 also resulted in significant inhibition of tumor growth (Fig. 8a–c). By Day 32, we sacrificed all mice ( $n = 7$ ) and found only trace amount of tumor tissue under the skin of mice treated with CARG-2020 (Fig. 8c). In another study, we also observed successful anti-tumoral effect of CARG-2020 by modulating the immune response in a syngeneic mouse model of recurrent ovarian cancer (Alvero and Mor, unpublished data). In a B16-F10 melanoma mouse model just as in the case of MC38 model, several doses of CARG-2020 are necessary in order to effectively eradicate established tumors (Wang et al., unpublished data). Taken together, it appears that CARG-2020 has been designed in such a way that multiple escape pathways adopted by tumors are targeted resulting in the prevention of tumor recurrence.

## 4. Discussion

The recent success of mRNA-based coronavirus vaccines in the clinic has solidified RNA as an alternative platform for cancer immunotherapy; however, the appeal of RNA-mediated gene targeting is presently hampered by delivery challenges<sup>61–64</sup>. Here we demonstrate that VLVs can be used to overcome the delivery issues of RNA. The ability of VLVs to carry multiple RNA sequences makes them attractive for use in cancer therapy. In addition, VLVs show oncolytic activity. VLVs are membrane encapsulated RNA replicons with a single structural protein VSV-G that can propagate in, and selectively kill PKR signaling defective cancer cells<sup>65,66</sup>. VLVs can be delivered systemically or locoregionally and therefore have the potential to act at both primary and metastatic tumor sites. Upon entry into cancer cells, VLV RNA replicons express their RNA cargo with rapid kinetics in the cytoplasm. On the contrary, DNA-based oncolytic viruses such as HSV and adenovirus which are in advanced stage of clinical development or are being marketed as oncotherapy viruses

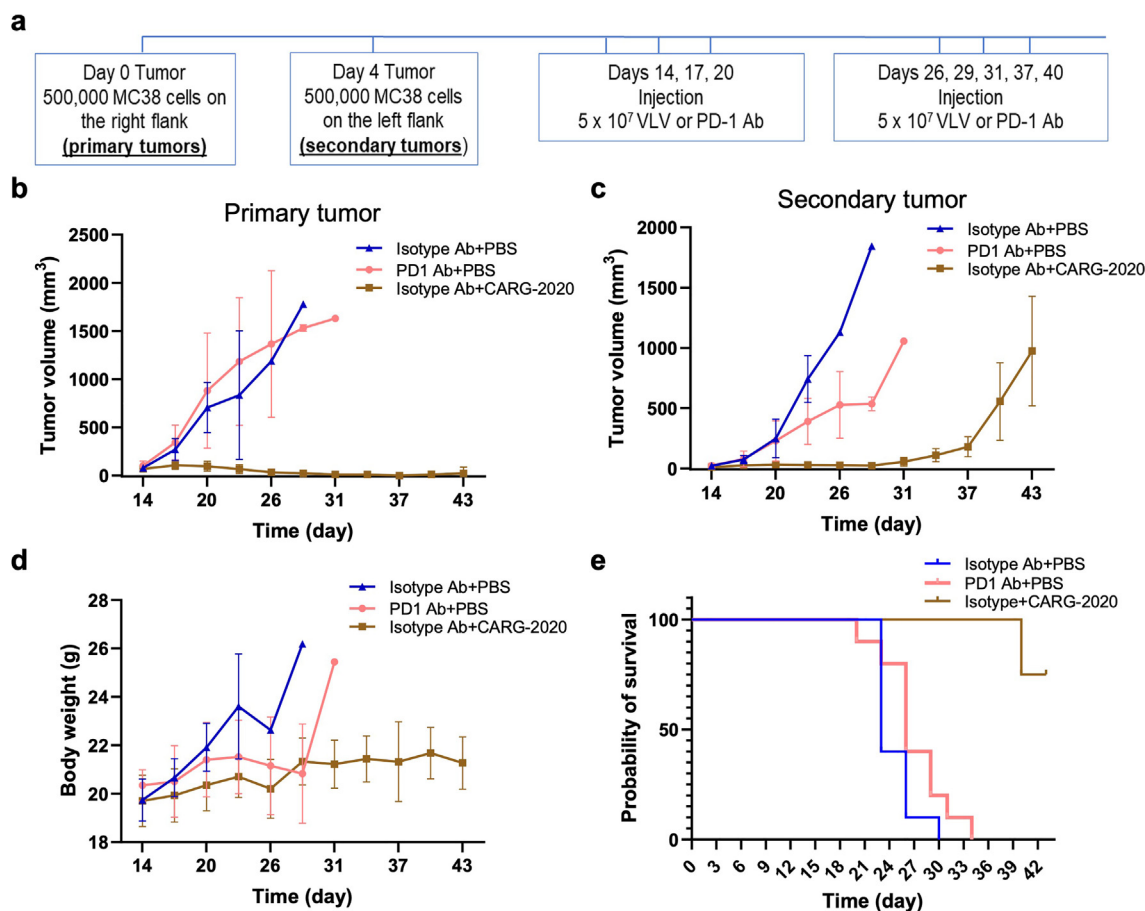


**Figure 7** CARG-2020 is superior to PD-1 antibody in primary and distant tumors and changes the immune status of noninjected tumors. (a) MC38 tumors were grafted to C57BL/6 mice on Day 0 (primary tumor) and Day 4 (secondary tumor), on the two flanks.  $5 \times 10^7$  pfu CARG-2020 were injected intratumorally to the primary tumors, and PD-1 blocking antibody were injected i.p. on indicated dates. Isotype antibody was used as a control for anti-PD-1, and PBS intratumoral injection was used as a control for CARG-2020. (b, c) Average sizes of primary (b) and secondary (c) tumors in mice treated with indicated agents. (d) Average body weights of mice treated with indicated agents. (e) Percentage of mice surviving under the treatment of indicated agents.

are ultimately dependent on the specific interactions between nuclear transcriptional factors of the tumors they infect and the DNA virus gene.

Tumors have become adept at employing panoply of escape mechanisms which are acquired through the accumulation of genetic mutations and epigenetic alterations<sup>67–69</sup>. Therefore, a multipronged approach targeting simultaneously several escape strategies is a rational approach to improving the efficacy of cancer immunotherapy. Conceptually, the three combined genetic approaches we have employed to generate CARG-2020 in this study may act in a mutually reinforcing manner to prevent tumor recurrence. First, by genetically linking p35 and p40 subunits with a flexible linker, we have “forced” the tethered subunits to be expressed together, potentially favoring the antitumor signaling properties of IL-12. This manipulation may also prevent increased *in vivo* competition for other subunits such as EB13 and thereby inhibit Treg pathway which promotes tumor growth<sup>70</sup>. Second, we have designed an IL-17 receptor A extracellular domain (IL-17RA-ECD) lacking the intracellular domain. The expressed IL-17RA ECD serves as a surrogate receptor for IL-17 binding and thereby blocks IL-17RA signaling and prevents it from fostering a tumor-promoting environment. Third, shRNA-mediated downregulation of PD-L1 in tumor cells can inhibit

cancer cell growth by enhancing immune responses. PD-L1 is expressed by diverse cell types in the CRC TME, and high levels of PD-L1 expression dampens antitumor immunity. The PD-1/PD-L1 axis exerts a crucial role in regulating Treg development in TME<sup>71</sup>. Systemic delivery of checkpoint inhibitors, such as anti-PD-1 or anti-PD-L1 antibodies, carries the risk of severe adverse effects<sup>72</sup>. The safety concerns are obviated by the use of shRNA which is more efficient than small molecules or antibody blockade in turning off PD-L1 expression resulting in low protein production. Our individual payload VLV showed a certain level of efficacy but is insufficient to control the tumor but when combined as CARG-2020, acts in concert to regress tumor more effectively and to prevent its recurrence.

Our gene profiling data particularly on oncogenic pathways, pro-inflammatory and immune suppressive molecules in the TME corroborate the notion that both CARG-2020 and VLV-IL-12 foster different TMEs (Fig. 6). We found that VLV-IL-12-treated tumors display a more active immune suppressive network compared to CARG-2020. Particularly, high levels of certain cytokines (*e.g.*, IL-6, TGF- $\beta$ , and IL-10) may allow the generation of MDSCs that render tumors non-responsive<sup>73–77</sup>. These cytokines are abundant in VLV-IL-12 treated tumors but occur in negligible amounts in CARG-2020 therapy. This observation is correlated

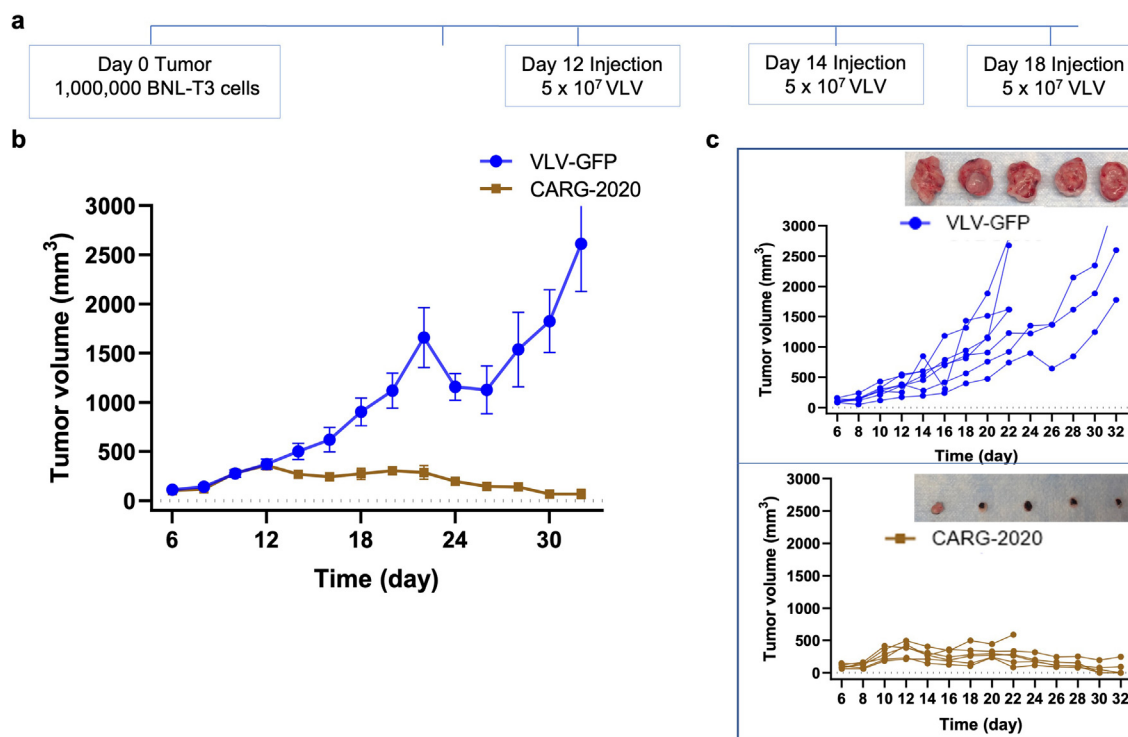


**Figure 8** CARG-2020 effectively targets BNL-T3 mouse liver tumors. (a)  $1 \times 10^6$  BNL-T3 cells were injected subcutaneously into BALB/c mice on Day 0. On Days 12, 14, and 18, tumors were injected with VLV-GFP, or CARG-2020 at a dose of  $5 \times 10^7$  pfu. (b, c) Average tumor volumes (b) and individual tumor volumes (c) were measured and calculated as described previously. Images of dissected subcutaneous tumors at the end of the study (Day 32) were shown as insets in (c)  $N = 7$  for VLV-IL-12;  $n = 6$  for CARG-2020. Data represent means  $\pm$  SEM for (b).

with the higher expression of a set of important co-stimulatory markers that help to maintain the active immune environment in CARG-2020-treated tumors than VLV-IL-12. The upregulation of the expression of co-stimulatory molecules is consistent with that described by others and is predictive of a more positive clinical outcome<sup>78</sup>. In contrast to CARG-2020 therapy, VLV-IL-12 therapy displays a slightly lower co-stimulatory immune environment with concomitant elevated expression levels of exhaustion markers (PD-L1/2, PD-1, and CTLA4). Overexpression of these markers in VLV-IL-12-treated tumors may render a rather active immune environment exhausted and thereby allowing tumors to recur after 33 days post-treatment. However, in CARG-2020 VLV therapy, the level of exhaustion marker expression is reduced and helps to maintain the active immune memory required to prevent tumor recurrence. The presence of downstream inflammatory signaling markers of the IL-17A pathway such as CXCL1, CXCL2, and other molecules supports the notion that an active inflammatory network is present in VLV-IL-12-treated tumors. This active inflammatory network, (a) up-regulates inhibitory molecules on antigen-presenting cells and tumor-associated macrophages, (b) inhibits T cell infiltration into the TME, and (c) converts otherwise sensitive tumors to be non-responsive to therapies<sup>27–30,79–84</sup>. Although VLV-IL-12 treatment resulted in impressive antitumor responses as evidenced by the prolongation of overall survival, it failed to prevent tumor relapse. It is not surprising that IL-12 stand-alone therapies have so far failed to advance in the clinic despite the impressive data accumulated in mice<sup>85</sup>. It is tempting to speculate that IL-12 VLVs altered the TME to enhance immunogenicity which we further exploited through the use of immune checkpoint blockade and dn-IL-17RA

to augment antitumor responses and prevent recurrence. The lack of tumor recurrence is correlated with the significant down-regulation of CRC stem cell and metastasis markers in CARG-2020 treated tumors (Fig. 6e).

Our results demonstrate proof of concept for the use of CARG-2020 in cancer immunotherapy. The tumor cell challenge studies show no tumor growth in CARG-2020 treated group supporting the notion that a combination of three immunomodulatory is effective in generating a strong immunological memory compared to VLV-IL-12 (Fig. 2e). This strong immunological memory generated at primary tumor acts not only to suppress the tumor but also distant secondary tumors (Fig. 4). Although the exact mechanism of prevention of tumor recurrence remains to be elucidated, gene expression signatures in the tumor tissue suggests that CARG-2020 suppresses the activity of cancer-promoting inflammation, cancer stemness, and oncogenic pathways compared to IL-12-expressing VLV. It is apparent that expressing IL-12, IL-17RA antagonist, and shRNA for PD-L1 is necessary for tumoricidal activity, but each alone is not sufficient to prevent tumor recurrence. However, when they are co-expressed in CARG-2020 VLV they act synergistically to prevent tumor recurrence. Gene expression profile data also suggest that CARG-2020 therapy prevents immune cell exhaustion and maintains active immunological memory in the TME. Recent studies have shown a synergistic effect of IL-17 blockade when combined with anti-PD-1 therapy, thus reiterating the potential of targeting IL-17 for the improvement of cancer immunotherapy<sup>86–88</sup>, especially when combined with other immune pathway blockers.

The VLV platform shows promise as a safe and effective cancer immunotherapy approach. VLVs are inherently safe due to



restriction of their replication by type I IFN<sup>89,90</sup>. The bio-distribution studies support CARG-2020 as a safe biologic, and its expression mostly confined to tumor site. While systemic delivery of cytokines such as IL-12, or checkpoint inhibitors such as anti-PD-1 or anti-PD-L1 antibodies carry risks of severe adverse effects, VLV-mediated intratumoral delivery of IL-12 and shRNA for PD-L1 is likely to be safer due to localized and transient expression of the payload.

We acknowledge that there are several limitations to this study that prevent the full profiling of this oncolytic virus therapy. First, the contribution of each of the transgenes to adaptive immunity needs to be examined through detailed gene expression analysis and T cell receptor repertoire analysis. Second, we have demonstrated that the immune status changes in tumor TMEs triggered by CARG-2020 and VLV-IL-12 by characterizing the molecular markers of TME. However, it would be important to further investigate the behavior and roles of various tumor-infiltrating cells, including Treg cells, antigen-presenting cells, and stromal cells<sup>91</sup>, considering the anticipated broad applicability of this oncolytic virus therapy. Third, it is necessary to elucidate what types of tumors are expected to be more sensitive to this therapy by developing panels of biomarkers. Although CARG-2020 payloads by i.t. injection is principally found at the site of injection (i.e., tumor) with little dissemination to other tissues and organs, we have not assessed whether CARG-2020 is capable of locally releasing proteins and cytokines (IL-12 and dn-IL17RA) from TME into the different tissues and organs, while minimizing systemic exposure.

### Acknowledgments

This work was supported by an American Association of Immunologists Careers in Immunology Fellowship to Ju Chen, University of Connecticut Innovation Fund to Valerian Nakaar and Kepeng Wang, and National Institute of Health/National Cancer Institute (NIH/NCI R01CA262430, USA) to Kepeng Wang. This research was also funded by NIDDK (Nos. R43DK113858 and R44DK113858, USA) and by NIAID (No. R43AI149798, USA) to Valerian Nakaar. The content is solely the responsibility of the authors and does not necessarily represent the official views of the National Institutes of Health. The funders had no role in study design, data collection and interpretation, or the decision to submit the work for publication.

### Author contributions

Ju Chen, Bhaskara Reddy Madina, Xian-Yong Ma, Bijan Almassian, Valerian Nakaar, and Kepeng Wang conceived this project. Ju Chen, Bhaskara Reddy Madina, Elham Ahmadi, Marie Marthe Krady, Eileen Victoria Meehan, Isabella China Wang, Xiaoyang Ye, Elise Pitmon, and Xian-Yong Ma performed the experiments and analyzed the data. Timur Olegovich Yarovinsky provided conceptual advice and analyzed the data. Ju Chen, Bhaskara Reddy Madina, Timur Olegovich Yarovinsky, Valerian Nakaar, and Kepeng Wang wrote the manuscript, with all authors contributing to the writing, editing, and providing key advice.

### Conflicts of interest

Kepeng Wang is a member of the Scientific Advisory Board of CaroGen Corporation. Bhaskara Reddy Madina, Elham Ahmadi,

Timur Olegovich Yarovinsky, Marie Marthe Krady, Xian-Yong Ma, Valerian Nakaar, and Bijan Almassian are current or former employees of CaroGen Corporation. The authors have no additional financial interests.

### Appendix A. Supporting information

Supporting data to this article can be found online at <https://doi.org/10.1016/j.apsb.2023.08.034>.

### References

- Pardoll DM. The blockade of immune checkpoints in cancer immunotherapy. *Nat Rev Cancer* 2012;**12**:252–64.
- Egen JG, Ouyang W, Wu LC. Human anti-tumor immunity: insights from immunotherapy clinical trials. *Immunity* 2020;**52**:36–54.
- Macedo N, Miller DM, Haq R, Kaufman HL. Clinical landscape of oncolytic virus research in 2020. *J Immunother Cancer* 2020;**8**:e001486.
- Alberts P, Tilgase A, Rasa A, Bandere K, Venskus D. The advent of oncolytic virotherapy in oncology: the Rigvir(R) story. *Eur J Pharmacol* 2018;**837**:117–26.
- Liang M. Oncorine, the world first oncolytic virus medicine and its update in China. *Curr Cancer Drug Targets* 2018;**18**:171–6.
- Andtbacka RH, Kaufman HL, Collichio F, Amatruda T, Senzer N, Chesney J, et al. Talimogene laherparepvec improves durable response rate in patients with advanced melanoma. *J Clin Oncol* 2015;**33**:2780–8.
- Rolls MM, Webster P, Balba NH, Rose JK. Novel infectious particles generated by expression of the vesicular stomatitis virus glycoprotein from a self-replicating RNA. *Cell* 1994;**79**:497–506.
- Rose NF, Publicover J, Chattopadhyay A, Rose JK. Hybrid alphavirus-rhabdovirus propagating replicon particles are versatile and potent vaccine vectors. *Proc Natl Acad Sci U S A* 2008;**105**:5839–43.
- Rose NF, Buonocore L, Schell JB, Chattopadhyay A, Bahl K, Liu X, et al. *In vitro* evolution of high-titer, virus-like vesicles containing a single structural protein. *Proc Natl Acad Sci U S A* 2014;**111**:16866–71.
- Chiale C, Yarovinsky TO, Mason SW, Madina BR, Menon M, Krady MM, et al. Modified alphavirus-vesiculovirus hybrid vaccine vectors for homologous prime-boost immunotherapy of chronic hepatitis B. *Vaccines* 2020;**8**:279.
- Rolls MM, Haglund K, Rose JK. Expression of additional genes in a vector derived from a minimal RNA virus. *Virology* 1996;**218**:406–11.
- Reynolds TD, Buonocore L, Rose NF, Rose JK, Robek MD. Virus-like vesicle-based therapeutic vaccine vectors for chronic hepatitis B virus infection. *J Virol* 2015;**89**:10407–15.
- Yarovinsky TO, Mason SW, Menon M, Krady MM, Haslip M, Madina BR, et al. Virus-like vesicles expressing multiple antigens for immunotherapy of chronic hepatitis B. *iScience* 2019;**21**:391–402.
- Schell JB, Rose NF, Bahl K, Diller K, Buonocore L, Hunter M, et al. Significant protection against high-dose simian immunodeficiency virus challenge conferred by a new prime-boost vaccine regimen. *J Virol* 2011;**85**:5764–72.
- Ribas A, Wolchok JD. Cancer immunotherapy using checkpoint blockade. *Science* 2018;**359**:1350–5.
- Larkin J, Chiarion-Sileni V, Gonzalez R, Grob JJ, Cowey CL, Lao CD, et al. Combined nivolumab and ipilimumab or monotherapy in untreated melanoma. *N Engl J Med* 2015;**373**:23–34.
- Arora SP, Mahalingam D. Immunotherapy in colorectal cancer: for the select few or all?. *J Gastrointest Oncol* 2018;**9**:170–9.
- Le DT, Uram JN, Wang H, Bartlett BR, Kemberling H, Eyring AD, et al. PD-1 blockade in tumors with mismatch-repair deficiency. *N Engl J Med* 2015;**372**:2509–20.
- Zou W, Wolchok JD, Chen L. PD-L1 (B7-H1) and PD-1 pathway blockade for cancer therapy: mechanisms, response biomarkers, and combinations. *Sci Transl Med* 2016;**8**:328rv4.

20. Topalian SL, Hodi FS, Brahmer JR, Gettinger SN, Smith DC, McDermott DF, et al. Safety, activity, and immune correlates of anti-PD-1 antibody in cancer. *N Engl J Med* 2012;**366**:2443–54.
21. Chen J, Pitmon E, Microbiome Wang K. Inflammation and colorectal cancer. *Semin Immunol* 2017;**32**:43–53.
22. Greten FR, Grivnenkov SI. Inflammation and cancer: triggers, mechanisms, and consequences. *Immunity* 2019;**51**:27–41.
23. Ma S, Cheng Q, Cai Y, Gong H, Wu Y, Yu X, et al. IL-17A produced by gammadelta T cells promotes tumor growth in hepatocellular carcinoma. *Cancer Res* 2014;**74**:1969–82.
24. Gomes AL, Teixeira A, Buren S, Tummala KS, Yilmaz M, Waisman A, et al. Metabolic inflammation-associated IL-17A causes non-alcoholic steatohepatitis and hepatocellular carcinoma. *Cancer Cell* 2016;**30**:161–75.
25. Zhuang Y, Peng LS, Zhao YL, Shi Y, Mao XH, Chen W, et al. CD8<sup>+</sup> T cells that produce interleukin-17 regulate myeloid-derived suppressor cells and are associated with survival time of patients with gastric cancer. *Gastroenterology* 2012;**143**:951–62. e8.
26. Wu S, Rhee KJ, Albesiano E, Rabizadeh S, Wu X, Yen HR, et al. A human colonic commensal promotes colon tumorigenesis via activation of T helper type 17 T cell responses. *Nat Med* 2009;**15**:1016–22.
27. Coffelt SB, Kersten K, Doornebal CW, Weiden J, Vrijland K, Hau CS, et al. IL-17-producing gammadelta T cells and neutrophils conspire to promote breast cancer metastasis. *Nature* 2015;**522**:345–8.
28. Chen J, Ye X, Pitmon E, Lu M, Wan J, Jellison ER, et al. IL-17 inhibits CXCL9/10-mediated recruitment of CD8<sup>+</sup> cytotoxic T cells and regulatory T cells to colorectal tumors. *J Immunother Cancer* 2019;**7**:324.
29. Wang K, Kim MK, Di Caro G, Wong J, Shalpour S, Wan J, et al. Interleukin-17 receptor a signaling in transformed enterocytes promotes early colorectal tumorigenesis. *Immunity* 2014;**41**:1052–63.
30. Reppert S, Boross I, Koslowski M, Tureci O, Koch S, Lehr HA, et al. A role for T-bet-mediated tumour immune surveillance in anti-IL-17A treatment of lung cancer. *Nat Commun* 2011;**2**:600.
31. Bramson JL, Hitt M, Addison CL, Muller WJ, Gaudie J, Graham FL. Direct intratumoral injection of an adenovirus expressing interleukin-12 induces regression and long-lasting immunity that is associated with highly localized expression of interleukin-12. *Hum Gene Ther* 1996;**7**:1995–2002.
32. Hsieh CS, Macatonia SE, Tripp CS, Wolf SF, O'Garra A, Murphy KM. Development of TH1 CD4<sup>+</sup> T cells through IL-12 produced by *Listeria*-induced macrophages. *Science* 1993;**260**:547–9.
33. Manetti R, Gerosa F, Giudizi MG, Biagiotti R, Parronchi P, Piccinni MP, et al. Interleukin 12 induces stable priming for interferon gamma (IFN-gamma) production during differentiation of human T helper (Th) cells and transient IFN-gamma production in established Th2 cell clones. *J Exp Med* 1994;**179**:1273–83.
34. Watkins SK, Egilmez NK, Suttles J, Stout RD. IL-12 rapidly alters the functional profile of tumor-associated and tumor-infiltrating macrophages *in vitro* and *in vivo*. *J Immunol* 2007;**178**:1357–62.
35. Steding CE, Wu ST, Zhang Y, Jeng MH, Elzey BD, Kao C. The role of interleukin-12 on modulating myeloid-derived suppressor cells, increasing overall survival and reducing metastasis. *Immunology* 2011;**133**:221–38.
36. Smith SG, Baltz JL, Koppolu BP, Ravindranathan S, Nguyen K, Zaharoff DA. Immunological mechanisms of intravesical chitosan/interleukin-12 immunotherapy against murine bladder cancer. *Oncol Immunology* 2017;**6**:e1259050.
37. Zhao J, Zhao J, Perlman S. Differential effects of IL-12 on Tregs and non-Treg T cells: roles of IFN-gamma, IL-2 and IL-2R. *PLoS One* 2012;**7**:e46241.
38. Kerkar SP, Goldszmid RS, Muranski P, Chinnasamy D, Yu Z, Reger RN, et al. IL-12 triggers a programmatic change in dysfunctional myeloid-derived cells within mouse tumors. *J Clin Invest* 2011;**121**:4746–57.
39. Buszello H. Antiproliferative effects of four different cytokines on renal carcinoma cell lines. *Anticancer Res* 1995;**15**:735–8.
40. Wall L, Burke F, Barton C, Smyth J, Balkwill F. IFN-gamma induces apoptosis in ovarian cancer cells *in vivo* and *in vitro*. *Clin Cancer Res* 2003;**9**:2487–96.
41. Voest EE, Kenyon BM, O'Reilly MS, Truitt G, D'Amato RJ, Folkman J. Inhibition of angiogenesis *in vivo* by interleukin 12. *J Natl Cancer Inst* 1995;**87**:581–6.
42. Saiki I, Sato K, Yoo YC, Murata J, Yoneda J, Kiso M, et al. Inhibition of tumor-induced angiogenesis by the administration of recombinant interferon-gamma followed by a synthetic lipid-A subunit analogue (GLA-60). *Int J Cancer* 1992;**51**:641–5.
43. Boehm U, Klamp T, Groot M, Howard JC. Cellular responses to interferon-gamma. *Annu Rev Immunol* 1997;**15**:749–95.
44. Colombo MP, Trinchieri G. Interleukin-12 in anti-tumor immunity and immunotherapy. *Cytokine Growth Factor Rev* 2002;**13**:155–68.
45. Vizler C, Rosato A, Calderazzo F, Quintieri L, Fruscella P, Wainstok de Calmanovici R, et al. Therapeutic effect of interleukin 12 on mouse haemangiosarcomas is not associated with an increased anti-tumour cytotoxic T-lymphocyte activity. *Br J Cancer* 1998;**77**:656–62.
46. Noguchi Y, Jungbluth A, Richards EC, Old LJ. Effect of interleukin 12 on tumor induction by 3-methylcholanthrene. *Proc Natl Acad Sci U S A* 1996;**93**:11798–801.
47. Zaharoff DA, Hance KW, Rogers CJ, Schlom J, Greiner JW. Intratumoral immunotherapy of established solid tumors with chitosan/IL-12. *J Immunother* 2010;**33**:697–705.
48. Smyth MJ, Taniguchi M, Street SE. The anti-tumor activity of IL-12: mechanisms of innate immunity that are model and dose dependent. *J Immunol* 2000;**165**:2665–70.
49. Brunda MJ, Luistro L, Warriar RR, Wright RB, Hubbard BR, Murphy M, et al. Antitumor and antimetastatic activity of interleukin 12 against murine tumors. *J Exp Med* 1993;**178**:1223–30.
50. Nguyen KG, Vrabel MR, Mantooth SM, Hopkins JJ, Wagner ES, Gabaldon TA, et al. Localized interleukin-12 for cancer immunotherapy. *Front Immunol* 2020;**11**:575597.
51. Tugues S, Burkhard SH, Ohs I, Vrohings M, Nussbaum K, Vom Berg J, et al. New insights into IL-12-mediated tumor suppression. *Cell Death Differ* 2015;**22**:237–46.
52. Lyster HK, Osada T, Hartman ZC. Right time and place for IL12: targeted delivery stimulates immune therapy. *Clin Cancer Res* 2019;**25**:9–11.
53. Osada T, Berglund P, Morse MA, Hubby B, Lewis W, Niedzwiecki D, et al. Co-delivery of antigen and IL-12 by Venezuelan equine encephalitis virus replicon particles enhances antigen-specific immune responses and antitumor effects. *Cancer Immunol Immunother* 2012;**61**:1941–51.
54. Quetglas JI, Labiano S, Aznar MA, Bolanos E, Azpilikueta A, Rodriguez I, et al. Virotherapy with a semliki forest virus-based vector encoding IL12 synergizes with PD-1/PD-L1 blockade. *Cancer Immunol Res* 2015;**3**:449–54.
55. Jiang C, Magee DM, Cox RA. Construction of a single-chain interleukin-12-expressing retroviral vector and its application in cytokine gene therapy against experimental coccidioidomycosis. *Infect Immun* 1999;**67**:2996–3001.
56. Liu S, Song X, Chrnyk BA, Shanker S, Hoth LR, Marr ES, et al. Crystal structures of interleukin 17A and its complex with IL-17 receptor A. *Nat Commun* 2013;**4**:1888.
57. Corbett TH, Griswold Jr DP, Roberts BJ, Peckham JC, Schabel Jr FM. Tumor induction relationships in development of transplantable cancers of the colon in mice for chemotherapy assays, with a note on carcinogen structure. *Cancer Res* 1975;**35**:2434–9.
58. Tanaka A, Sakaguchi S. Regulatory T cells in cancer immunotherapy. *Cell Res* 2017;**27**:109–18.
59. Togashi Y, Shitara K, Nishikawa H. Regulatory T cells in cancer immunosuppression—implications for anticancer therapy. *Nat Rev Clin Oncol* 2019;**16**:356–71.
60. Aihara A, Huang CK, Olsen MJ, Lin Q, Chung W, Tang Q, et al. A cell-surface beta-hydroxylase is a biomarker and

- therapeutic target for hepatocellular carcinoma. *Hepatology* 2014;**60**:1302–13.
61. Fiedler K, Lazzaro S, Lutz J, Rauch S, Heidenreich R. mRNA cancer vaccines. *Recent Results Cancer Res* 2016;**209**:61–85.
  62. Gao Y, Men K, Pan C, Li J, Wu J, Chen X, et al. Functionalized DMP-039 hybrid nanoparticle as a novel mRNA vector for efficient cancer suicide gene therapy. *Int J Nanomed* 2021;**16**:5211–32.
  63. Tang X, Zhang S, Fu R, Zhang L, Huang K, Peng H, et al. Therapeutic prospects of mRNA-based gene therapy for glioblastoma. *Front Oncol* 2019;**9**:1208.
  64. Liang X, Li D, Leng S, Zhu X. RNA-based pharmacotherapy for tumors: from bench to clinic and back. *Biomed Pharmacother* 2020;**125**:109997.
  65. Schreiber LM, Urbiola C, Das K, Spiesschaert B, Kimpel J, Heinemann F, et al. The lytic activity of VSV-GP treatment dominates the therapeutic effects in a syngeneic model of lung cancer. *Br J Cancer* 2019;**121**:647–58.
  66. Gaddy DF, Lyles DS. Oncolytic vesicular stomatitis virus induces apoptosis via signaling through PKR, Fas, and Daxx. *J Virol* 2007;**81**:2792–804.
  67. Yamashita S, Kishino T, Takahashi T, Shimazu T, Charvat H, Kakugawa Y, et al. Genetic and epigenetic alterations in normal tissues have differential impacts on cancer risk among tissues. *Proc Natl Acad Sci U S A* 2018;**115**:1328–33.
  68. Stewart TJ, Abrams SI. How tumours escape mass destruction. *Oncogene* 2008;**27**:5894–903.
  69. Whiteside TL, Mandapathil M, Szczepanski M, Szajnik M. Mechanisms of tumor escape from the immune system: adenosine-producing Treg, exosomes and tumor-associated TLRs. *Bull Cancer* 2011;**98**:E25–31.
  70. Liao KL, Bai XF, Friedman A. Mathematical modeling of Interleukin-35 promoting tumor growth and angiogenesis. *PLoS One* 2014;**9**:e110126.
  71. Han Y, Liu D, Li L. PD-1/PD-L1 pathway: current researches in cancer. *Am J Cancer Res* 2020;**10**:727–42.
  72. Su C, Wang H, Liu Y, Guo Q, Zhang L, Li J, et al. Adverse effects of anti-PD-1/PD-L1 therapy in non-small cell lung cancer. *Front Oncol* 2020;**10**:554313.
  73. Guerrouahen BS, Maccalli C, Cugno C, Rutella S, Akporiaye ET. Reverting immune suppression to enhance cancer immunotherapy. *Front Oncol* 2019;**9**:1554.
  74. Zhao H, Wu L, Yan G, Chen Y, Zhou M, Wu Y, et al. Inflammation and tumor progression: signaling pathways and targeted intervention. *Signal Transduct Targeted Ther* 2021;**6**:263.
  75. Taylor A, Verhagen J, Blaser K, Akdis M, Akdis CA. Mechanisms of immune suppression by interleukin-10 and transforming growth factor-beta: the role of T regulatory cells. *Immunology* 2006;**117**:433–42.
  76. Battle E, Massague J. Transforming growth factor-beta signaling in immunity and cancer. *Immunity* 2019;**50**:924–40.
  77. Yang Y, Li C, Liu T, Dai X, Bazhin AV. Myeloid-derived suppressor cells in tumors: from mechanisms to antigen specificity and micro-environmental regulation. *Front Immunol* 2020;**11**:1371.
  78. Capece D, Verzella D, Fischietti M, Zazzeroni F, Alesse E. Targeting costimulatory molecules to improve antitumor immunity. *J Biomed Biotechnol* 2012;**2012**:926321.
  79. Zhao J, Chen X, Herjan T, Li X. The role of interleukin-17 in tumor development and progression. *J Exp Med* 2020;**217**:e20190297.
  80. He D, Li H, Yusuf N, Elmets CA, Li J, Mountz JD, et al. IL-17 promotes tumor development through the induction of tumor promoting microenvironments at tumor sites and myeloid-derived suppressor cells. *J Immunol* 2010;**184**:2281–8.
  81. Gonzalez H, Hagerling C, Werb Z. Roles of the immune system in cancer: from tumor initiation to metastatic progression. *Genes Dev* 2018;**32**:1267–84.
  82. Grivnickov SI, Greten FR, Karin M. Immunity, inflammation, and cancer. *Cell* 2010;**140**:883–99.
  83. Xiang X, Wang J, Lu D, Xu X. Targeting tumor-associated macrophages to synergize tumor immunotherapy. *Signal Transduct Targeted Ther* 2021;**6**:75.
  84. Rabinovich GA, Gabrilovich D, Sotomayor EM. Immunosuppressive strategies that are mediated by tumor cells. *Annu Rev Immunol* 2007;**25**:267–96.
  85. Lasek W, Zagozdzon R, Jakobisiak M. Interleukin 12: still a promising candidate for tumor immunotherapy?. *Cancer Immunol Immunother* 2014;**63**:419–35.
  86. Li Q, Ngo PT, Egilmez NK. Anti-PD-1 antibody-mediated activation of type 17 T-cells undermines checkpoint blockade therapy. *Cancer Immunol Immunother* 2020;**70**:1789–96.
  87. Zhang Y, Chandra V, Riquelme Sanchez E, Dutta P, Quesada PR, Rakoski A, et al. Interleukin-17-induced neutrophil extracellular traps mediate resistance to checkpoint blockade in pancreatic cancer. *J Exp Med* 2020;**217**:e20190354.
  88. Nagaoka K, Shirai M, Taniguchi K, Hosoi A, Sun C, Kobayashi Y, et al. Deep immunophenotyping at the single-cell level identifies a combination of anti-IL-17 and checkpoint blockade as an effective treatment in a preclinical model of data-guided personalized immunotherapy. *J Immunother Cancer* 2020;**8**:e001358.
  89. van den Pol AN, Mao G, Chattopadhyay A, Rose JK, Davis JN. Chikungunya, influenza, nipah, and semliki forest chimeric viruses with vesicular stomatitis virus: actions in the brain. *J Virol* 2017;**91**:e02154-16.
  90. Marchese AM, Chiale C, Moshkani S, Robek MD. Mechanisms of innate immune activation by a hybrid Alphavirus–Rhabdovirus vaccine platform. *J Interferon Cytokine Res* 2020;**40**:92–105.
  91. Ilkow CS, Marguerie M, Batenchuk C, Mayer J, Ben Neriah D, Cousineau S, et al. Reciprocal cellular cross-talk within the tumor microenvironment promotes oncolytic virus activity. *Nat Med* 2015;**21**:530–6.